Glycobiology vol. 10 no. 11 pp. 1147–1156, 2000

Conformation and dynamics of heparin and heparan sulfate

Barbara Mulloy[1] and Mark J.Forster

National Institute for Biological Standards and Control, Blanche Lane, South Mimms, Potters Bar, Hertfordshire EN6 3QG, UK

Accepted on July 27, 2000

The glycosaminoglycans heparin and heparan sulfate contain similar structural units in varying proportions providing considerable diversity in sequence and biological function. Both compounds are alternating copolymers of glucosamine with both iduronate- and glucuronate-containing sequences bearing *N*-sulfate, *N*-acetyl, and *O*-sulfate substitution. Protein recognition of these structurally-diverse compounds depends upon substitution pattern, overall molecular shape, and on internal mobility. In this review particular attention is paid to the dynamic aspects of heparin/heparan sulfate conformation. The iduronate residue possesses an unusually flexible pyranose ring conformation. This extra source of internal mobility creates special problems in rationalization of experimental data for these compounds. We present herein the solution-state NMR parameters, fiber diffraction data, crystallographic data, and molecular modeling methods employed in the investigation of heparin and heparan sulfate. Heparin is a useful model compound for the sulfated, protein-binding regions of heparan sulfate. The literature contains a number of solution and solid-state studies of heparin oligo- and polysaccharides for both isolated heparin species and those bound to protein receptors. These studies indicate a diversity of iduronate ring conformations, but a limited range of glycosidic linkage geometries in the repeating disaccharides. In this sense, heparin exhibits a well-defined overall shape within which iduronate ring forms can freely interconvert. Recent work suggests that computational modeling could potentially identify heparin binding sites on protein surfaces.

Key words: heparin/heparan sulfate/conformational analysis

Introduction

The glycosaminoglycans (GAGs) are linear polysaccharides with alternating uronic acid and hexosamine residues, in which a limited set of monosaccharide units gives rise to a number of complex sequences by variable substitution with *O*-sulfate, *N*-sulfate, and *N*-acetyl groups. GAGs usually exist as the O-linked side-chains of proteoglycans, displaying a set of physiological functions which is remarkably wide and as yet incompletely explored. They may act as structural components of connective tissue and the extracellular matrix, or as specific ligands in the relationship between the cell surface and its surroundings.

Table I presents a simplified summary of GAG structures. The galactosamine-containing GAGs are chondroitin-4-sulfate (chondroitin sulfate A), chondroitin-6-sulfate (chondroitin sulfate C), and dermatan sulfate, also known as chondroitin sulfate B. Glucosamine-containing GAGs include hyaluronan, heparin, and heparan sulfate. A closely related compound, keratan sulfate, contains no uronic acid but consists of a repeating poly-(*N*-acetyllactosamine) disaccharide sequence, usually with 6-O-sulfated GlcNAc and partially 6-O-sulfated Gal.

For a variety of reasons, heparin and heparan sulfate have attracted more physico-chemical interest than the other GAGs. Heparan sulfate exists on the surface of most or all mammalian cells and can display a remarkable range of different sequence motifs; its range of interactions and possible functions reflect its structural complexity. The main repeat unit of heparin structurally resembles the protein binding sequences in heparan sulfate, but contains a higher percentage of sulfated residues. Utilized therapeutically as an anticoagulant and readily available in good quantities, heparin serves as a useful model for heparan sulfate. Finally, heparin's highly-sulfated scaffold simplifies the study of its solution conformation by providing NMR spectra with enhanced dispersion properties as compared to those found with other GAGs.

In what sense can these linear polysaccharides display distinct conformational features? Unbranched, they cannot fold into anything resembling the tertiary structures of proteins, yet the specificity of their interactions with proteins suggests some level of structural definition. Lacking the variety of functional groups displayed by peptides, these anionic polysaccharides must provide a spatially defined pattern of sulfate and carboxylate substituents for molecular recognition to take place. All determinations of the conformation of heparin (both in solution and in the solid state) have indicated similar, well-defined molecular structures in terms of overall chain conformation, with additional subtlety arising from the conformational versatility of the pyranose ring of iduronic acid.

Theoretical and experimental approaches to conformation and molecular motion

The determination of three-dimensional structure in GAGs relies upon many of the same methods as those utilized in the investigation of other complex carbohydrates (Rao *et al.*, 1998). Researchers generally employ NMR spectroscopy and molecular modeling to generate detailed solution structures for

[1]To whom correspondence should be addressed

Table I. Main repeating structures in the glycosaminoglycans

Glycosaminoglycan	Synonym	Structure of main repeating disaccharide
Hyaluronan		-4)-β-D-GlcA-(1→3)-β-D-GlcNAc-(1-
Chondroitin-4-sulfate	Chondroitin sulfate A	-4)-β-D-GlcA-(1→3)-β-D-GalNAc4(OSO_3^-)-(1-
Chondroitin-6-sulfate	Chondroitin sulfate C	-4)-β-D-GlcA-(1→3)-β-D-GalNAc6(OSO_3^-)-(1-
Dermatan sulfate	Chondroitin sulfate B	-4)-α-L-IdoA-(1→3)-β-D-GalNAc4(OSO_3^-)-(1-
Heparin		-4)-α-L-IdoA2(OSO_3^-)-(1→4)-α-D-GlcNSO_3^-,6(OSO_3^-)-(1-
Heparan sulfate		-4)-β-D-GlcA-(1→4)-α-D-GlcNAc-(1-
Keratan sulfate		-3)-β-D-Gal-(1→4)-β-D-GlcNAc6(OSO_3^-)-(1-

these polysaccharides, as many NMR parameters directly reflect molecular conformation. Spin-spin coupling constants ($^3J_{H,H}$) between vicinal protons monitor ring conformation while nuclear Overhauser effects (NOEs) between protons on adjacent monosaccharide residues provide information on glycosidic linkage geometries. Systematic energy calculations over all values of the glycosidic torsional angles ϕ and ψ allow the prediction of favorable ring conformations and the comparison of theoretical and experimental NOEs (Figure 1). The recent book of Rao *et al.* (1998) makes reference to many further strategies for applying NMR and molecular modeling to conformational analysis of complex carbohydrates.

Structure determination methods such as NMR and x-ray crystallography typically make some use of molecular modeling methods by assuming standard values for bond lengths and angles during the refinement process. Perez *et al.* (1998) report a quantitative comparison of the applicability of molecular mechanics force-fields to carbohydrate modeling. They considered a total of 20 variants of program, functional form, parameter sets and solvation model against a set of seven test cases. Because of a lack of trusted experimental data with errors less than the simulated value, the emphasis of this work is on the relationship between force-fields, rather than on which methods provide the best overall description of carbohydrate conformation and energetics. This work also serves as a useful reference to the original literature for the development of each method, where comparisons with experimental or quantum mechanical data are used in deriving molecular mechanics parameters. Molecular mechanics force-fields do not always provide parameters for sulfated carbohydrates, but the literature outlines development of specialized parameters for the MM2 force-field (Ferro *et al.*, 1995a, 1997) and for the AMBER and CHARMm force-fields (Huige and Altona, 1995). Some groups have successfully used the CVFF force-field for studies of carbohydrates (Asensio *et al.*, 1995), but we have found that sulfate geometry is poorly reproduced. The all-atom force-field ESFF gives better sulfate geometries and Mikhailov *et al.* (1996) have used it to study heparin oligosaccharides. Molecular mechanics is an empirical discipline, and the degree to which force-field imperfections matter depends on the application. Sometimes adequate results may be obtained with crude molecular modeling techniques (Mulloy *et al.*, 1993).

For polysaccharides in general, and glycosaminoglycans in particular, one must consider molecular motion and flexibility within a discussion of molecular conformation, as the frequency, amplitude, and geometry of such motions directly affect the measured NMR spectroscopic parameters.

A formal description of molecular motions generally requires the use of a reorientational correlation function, or equivalently, a spectral density function. These functions describe the way in which any "memory" of initial orientation changes as a result of overall molecular reorientation, internal motions, etc., for any given vector in the molecular framework. Thus, the reorientational correlation function represents a time course for the loss of such orientational memory. Its value of one at time zero must decay to a value of zero over time; its exact form will depend upon the details of the motion and on the vector selected. One defines correlation time—the quantity most frequently used in discussing typical timescales for molecular motion—as the area under the correlation function. The spectral density function represents the frequency spectrum analogue of the reorientational correlation function; knowledge of one implies knowledge of the other.

When a rigid molecule tumbles isotropically in solution (approximating the behavior of a sphere), all possible vectors in the molecule behave equivalently. The correlation function is then typically a simple exponential decay and the spectral density is a Lorentzian function (Harris, 1986). For a rigid symmetric top molecule (approximating the behavior of an ellipsoid), the properties of a given vector will depend upon the reorientation rates about the axes parallel and perpendicular to the major top axis as well as on the angle between the major top axis and the vector (Harris, 1986). Overall reorientation typically occurs on the picosecond (ps) to nanosecond (ns) timescale.

Researchers often utilize the model free approach of Lipari and Szabo (1982a,b) to discuss fast internal molecular motions. Here, internal motion quickly reduces the value of the correlation function from its initial value of one to a "plateau" value less than one. This model-free approach utilizes the extent of internal motions, rather than the exact detail of their type, to determine the plateau value obtained. The slower process of overall tumbling in solution subsequently effects a further loss in orientational correlation. The validity of this approach requires a much faster timescale for any internal motions than for overall reorientation. Some carbohydrate studies (Catoire *et al.*, 1997) suggest that this is not always the case, in particular for changes in glycosidic linkage conformation across energy barriers between minima; small-amplitude changes in the same energy well, however, are predicted to be rapid (Rutherford *et al.*, 1993).

NMR spin relaxation studies serve as important tools for probing molecular motions because spin relaxation rates, such as ^{13}C T_1 and T_2 values and ^1H-^1H cross relaxation rates directly relate to spectral density functions (Harris, 1986). Hadjuk *et al.* (1993) have presented a brief and clear summary of the effect of picosecond timescale motions on NMR relaxation parameters in monosaccharides. Computer simulation methods such as molecular dynamics (McCammon and Harvey, 1987) can help to rationalize experimental data. Unfortunately, current computer systems can simulate only a few nanoseconds, thereby limiting the range of motions that can be studied.

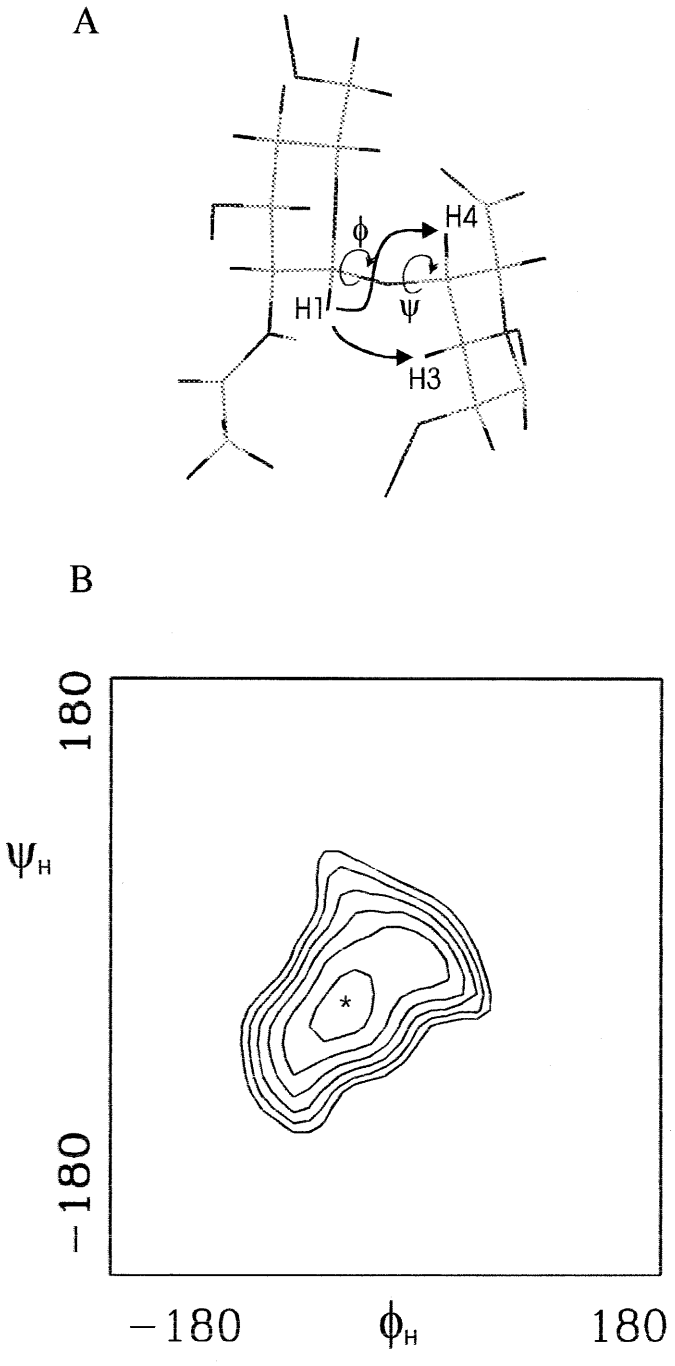

Fig. 1. (**A**) Diagram of the glycosidic linkage between GlcNAc and IdoA in a chemically-modified (*O*- and *N*- desulfated, re-*N*-acetylated) heparin (Mulloy *et al.*, 1994). The dihedral angles ϕ and ψ are indicated. Arrows mark observed inter-residue NOEs. (**B**) Contour plot in which total energy calculated in the AMBER forcefield is mapped against ϕ_H and ψ_H for GlcNAc-IdoA, where ϕ_H is defined by the atoms H1′-C1′-O4-C4 and ψ_H by C1′-O4-C4-H4. The minimum energy conformation marked * gives good agreement between predicted and measured NOEs, and is close to that for fully sulfated heparin. The geometry of glycosidic linkages in heparin is not determined by the presence or absence of sulfate substituents.

In the field of protein structure determination ^1H-^1H NOE and coupling constant data have traditionally been used to derive semi-quantitative distance and dihedral angle restraints (Wuthrich, 1986). These restraints are then used in a structure generation procedure that is based on either the distance geometry method (Wagner *et al.*, 1993) or a molecular dynamics simulation scheme (Brunger and Nilges, 1990). Typically these structure generation methods seek to find a single structure that is consistent with the restraints. If such a restraint-based single structure generation procedure is applied to carbohydrates, where multiple conformations may exist and contribute to the NMR data, then there is a danger that a non-physically realistic or virtual conformation might be obtained (Cumming and Carver, 1987). In analyzing GAG conformation and dynamics, the reorientation of a rigid body provides a starting point for the analysis, while rotation about the glycosidic linkage and the known flexibility of iduronate residues provide additional degrees of freedom. When such multiple conformations exist in solution the correct form of analysis depends upon the timescale of the conformer interchange. If changes in iduronate ring conformation or fluctuations in the torsion angles of glycosidic linkages consist of fast oscillations within a given energy well, then experience suggests that a Lipari-Szabo model superimposed on a rigid body description of overall reorientation is a good approximation. Conversely, slow oscillations complicate the analysis—particularly of ^1H-^1H NOE data—by prohibiting a Lipari-Szabo approach. Analysis of NOE data in the presence of multiple solution conformations requires knowledge of the conformers themselves as well as some estimate of the timescale for their inter-conversion. For conformers that interconvert on a timescale much slower than molecular reorientation but much faster than NMR spin relaxation times (these typically range from milliseconds to seconds), the correct method of analysis requires computation of an averaged matrix of ^1H-^1H spin relaxation rate constants and its use in a multi-spin simulation of the NOE time course. Studies of a tetrasaccharide fragment from the cell wall polysaccharide of *Streptococcus mitis* J22 (Xu *et al.*, 1996) and the monosaccharide α-L-IdoA-OMe (Forster and Mulloy, 1994) describe such an approach.

Analysis of $^3J_{H,H}$ values is simpler; the experimentally observed value is an average over all conformations present. This picture proves reliable unless the motions are sufficiently slow that they are comparable with the inverse of chemical shift differences (i.e., on the millisecond to second timescale) at which point NMR spectral line broadening and/or distinct spectra for each species might be found (Harris, 1986).

The conformational plasticity of α-L-iduronic acid

The conversion of β-D-glucuronate to α-L-iduronate *in vivo* occurs after polymerization of the GAG chain; Hagner-McWhirter *et al.*

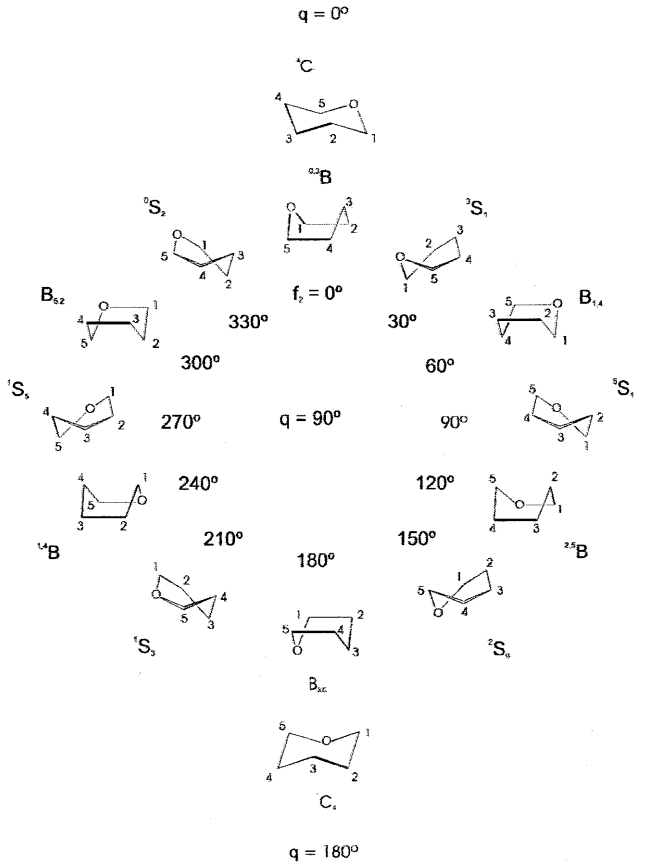

Fig. 2. Diagram of the conformational itinerary of the pyranose ring as defined by Jeffrey and Yates (1979) according to Cremer and Pople (1975). The canonical ring forms are represented on the surface of a sphere, with the $^4C_1$ and $^1C_4$ chairs at opposite poles ($\theta = 0°$ and 180°, respectively) and boat and skew-boat forms around the equator ($\theta = 90°$). Interconversion between the equatorial forms is referred to as pseudorotation. Reproduced from Forster and Mulloy (1993) with permission of John Wiley and Sons, Inc.

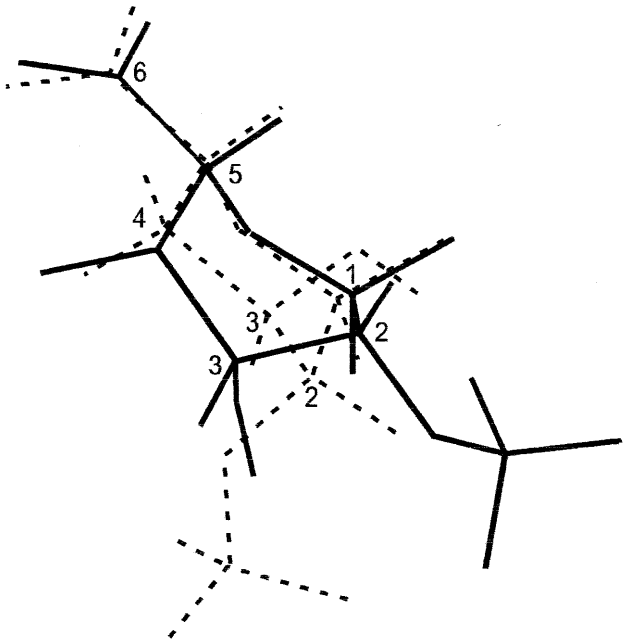

Fig. 3. Stick diagram of 2-*O*-sulfated iduronate, with the two pyranose ring forms ($^2S_0$, solid lines; $^1C_4$, broken lines) which contribute to the conformational equilibrium of internal iduronate residues in heparin overlaid. The change between the two forms can be accommodated with relatively modest changes to the geometry of linkages to adjacent residues, but there is a marked difference in the orientation of the sulfate substituent. Reproduced from Mulloy *et al.* (1994) with permission of Elsevier Science.

(2000) have described the specificity and mechanism of the C5 epimerase for heparin. This modification of the uronic acid residues, trivial as it may seem, profoundly affects the conformational and dynamic properties of the resulting polymer. All the D-galacto- and D-glucopyranose monosaccharide residues in GAGs are stable in the usual $^4C_1$ chair conformation of their six-membered pyranose rings. As with most other L-hexapyranoses, one might expect L-iduronate to adopt a $^1C_4$ chair as its most stable conformer. In fact, more than one solution conformation is accessible, and the equilibrium between them is readily altered. One can utilize proton NMR spectroscopy to track such ring geometries in some detail. Changes in the ring conformation not only alter the dihedral angles between vicinal hydrogen atoms, but also change the distances between hydrogens so that both spin-spin coupling constant ($^3J_{H,H}$) values and ^1H-^1H NOEs can effectively monitor ring shape. NMR studies of iduronate as a monosaccharide (Ferro *et al.*, 1990), or at the nonreducing end of oligosaccharides (Sanderson *et al.*, 1987; Ferro *et al.*, 1990), have given $^3J_{H,H}$ values which indicate a mixture of both the $^1C_4$ and $^4C_1$ chairs with an additional twisted conformation usually known as the $^2S_0$ skew-boat (Sanderson *et al.*, 1987; Ferro *et al.*, 1990). The diagram in Figure 2 shows a conformational itinerary for the pyranose ring illustrating all the canonical forms: the two chairs, six boats, and six skew boats. Internal iduronate residues in heparin adopt an equilibrium between two of these forms, the $^1C_4$ chair and the $^2S_0$ skew-boat (Ferro *et al.*, 1990). Figure 3 shows these two forms superimposed so that the C4-O4 and C1-O1 bonds are similar in their orientations. This demonstrates that the two forms may interconvert with little disturbance to glycosidic linkages to neighboring residues in the polysaccharide chain. The balance of the chair to skew-boat equilibrium in internal iduronate residues depends both upon its own substitution with 2-*O*-sulfate and on the substitution of adjacent glucosamine residues (van Boeckel *et al.*, 1987).

Ernst *et al.* (1998) have presented a graphical procedure for assessing physical data in terms of sterically accessible iduronate ring conformations. This procedure provides a qualitative assessment of the relative energetics of ring form interconversion pathways. They suggested that $^1C_4$ could most easily interchange with $^0S_2$ and $^3S_1$ forms, while $^4C_1$ could interchange with $^2S_0$ and $^1S_3$ forms. In addition, the interconversion between the $^2S_0$ and other boat and skew-boat forms (termed pseudorotation) seemed to be less hindered than chair-to-skew-boat changes.

Molecular dynamics simulations of iduronate (as the methyl glycoside and as the central residue of a trisaccharide) indicate that the pyranose ring may explore part of this conformational space on a rapid time-scale; the observed $^2S_0$ skew boat form

may represent an ensemble average over several closely-related conformations. Predicted ^{1}H-^{1}H NOE and $^3J_{H,H}$ values for the ensemble average compare closely with those for a static $^2S_0$ ring (Forster and Mulloy, 1994). Since the available coupling constant and NOE data could not distinguish between these two cases, it remains unclear whether extensive pseudorotation takes place in the methyl glycoside.

Studies of model compounds such as the neutral monosaccharide idose (Snyder and Serianni, 1986; Hadjuk *et al.*, 1993), or 1,2,3,4,6-penta-*O*-acetyl-α-D-idopyranose (Horita *et al.*, 1997), have shown that the interconversion rates between chair and skew-boat are slower than the rate of overall molecular reorientation.

Heparin

The NMR study of Gatti *et al.* (1979) indicated that the overall solution conformation of fully-sulfated, iduronate-containing regions of heparin might well resemble the earlier solid state structure of Atkins and Nieduszynski (1975). A later study confirmed this resemblance by analysis of inter-residue NOE measurements (Mulloy *et al.*, 1993). This study employed preparations of bovine lung heparin, which contains a high (>90%) proportion of the trisulfated disaccharide (Table I, Figure 4a). Similar studies have utilized a series of modified heparins, prepared from the same material, with systematically altered substitution patterns (Mulloy *et al.*, 1994). For all these heparin derivatives a distinctive pattern of intense inter-residue NOEs indicates relatively well-defined glycosidic linkages in iduronate containing sequences, as compared with those of other polysaccharides. (Mulloy *et al.*, 1993, 1994). The NOE data suggest occupation of a single area of low energy in the ϕ, φ map (see, for example, Figure 1). Surprisingly, all derivatives, regardless of sulfation pattern, exhibit similar glycosidic bond conformations but differ in the conformational equilibria of their iduronate residues. One heparin derivative in particular, de-*N*-sulfated, re-*N*-acetylated heparin, proved useful because internal iduronate residues exist almost entirely in the $^1C_4$ conformation (consistent with the results of van Boeckel *et al.* (1987) for oligosaccharides in which IdoA2OSO$_3$- is substituted at the 4-position by GlcNAc. Representation of this particular compound by a single molecular model allowed resolution of certain difficulties that had arisen in interpretation of NOE values. NOEs, like other relaxation phenomena, are a function of molecular motion (see *Theoretical and experimental approaches to conformation and molecular motion*). One cannot correctly predict the measured NOE values (even those within a single residue) assuming isotropic rotation for this system. However, assuming that heparin molecules behave as approximately cylindrical symmetric tops yields predicted NOEs close to experimental values (Forster *et al.*, 1989). Huckerby and Nieduszynski (1982) predicted this motional anisotropy on the basis of ^{13}C NMR relaxation parameters.

For heparin itself, one must consider the $^2S_0$ form of the iduronate ring, but a model in which heparin has a well-defined solution conformation (Figure 5) could readily accommodate both molecular mechanics calculations and inter-residue NOE values. The iduronate ring can change between $^1C_4$ and $^2S_0$ forms without causing the whole polysaccharide chain to bend.

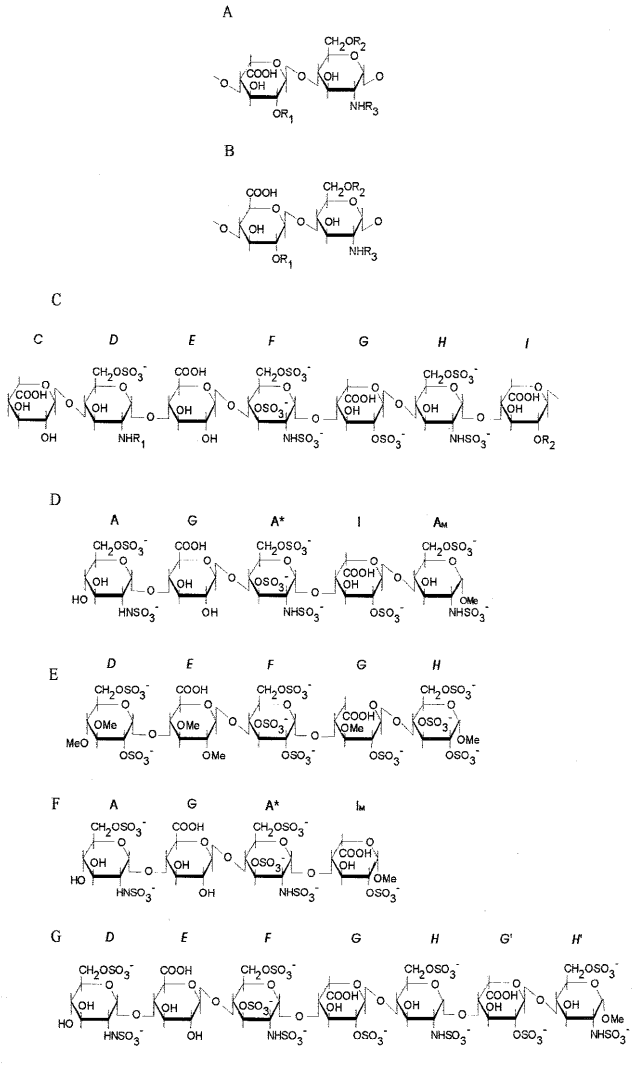

Fig. 4. Structures in heparin and heparan sulfate. (**A**) Generalized diagram of a heparin disaccharide: R_1 = SO_3- or H; R_2 = SO_3- or H; R_3 = SO_3- or $COCH_3$, and (**B**) Generalized diagram of a heparan sulfate disaccharide: R_1 = H or (rarely) SO_3-; R_2 = H or SO_3-; R_3 = $COCH_3$ or SO_3-. Samples of both heparin and heparan sulfate contain both types of structure; highly-sulfated, iduronate-containing sequences predominate in heparin, and occur occasionally in heparan sulfate. The sequence GlcNAc-IdoA is not produced in the biosynthesis of heparin or heparan sulfate. (**C**) The naturally occurring sequence in heparin and heparan sulfate with high affinity for antithrombin (Choay *et al.*, 1981). (**D**) A synthetic pentasaccharide, with high affinity for antithrombin, based on the central pentasaccharide of c) (Choay *et al.*, 1983). (**E**) A synthetic pentasaccharide which has been crystallized in complex with antithrombin (Jin *et al.*, 1997). (**F**) A tetrasaccharide with high affinity for antithrombin which has been the subject of NMR studies in solution alone and in the presence of antithrombin (Hricovini *et al.*, 1999). (**G**) A heptasaccharide related to c) by extension with an extra disaccharide at the reducing end, the subject of kinetic and molecular modeling studies (Belzar *et al.*, 2000).

Hricovini *et al.* (1995) have investigated the conformation and dynamics of a heparin epoxide using NMR relaxation data. A rigid body isotropic reorientation model cannot explain the NMR spin relaxation and ^{1}H-^{1}H NOE data, nor can an extension of such a model allowing fast internal motions using a model-free approach (Lipari and Szabo, 1982a). A symmetric top reorientation model, with internal motions on the picosecond

timescale, gives an improved fit to the data. This NMR study does not explicitly discuss the conformational properties of glycosidic linkages in this compound. Ferro *et al.* (1995b) have presented a molecular mechanics study of the same heparin epoxide using the MM2 force-field, showing the presence of several possible glycosidic torsion angle conformations for disaccharide models. Extending these calculations to models of higher oligomers indicates that they are more restricted. In a heptamer model ~90% of the population of each glycosidic linkage reflects a single linkage geometry, implying a relatively rigid, rod-like molecular shape which would reorient as a symmetric top in solution.

Conformations of heparin oligosaccharides

Heterogeneity and polydispersity of heparin polysaccharide can complicate the analysis of NMR data, but the preparation of homogeneous heparin oligosaccharides can overcome this problem. Investigators have performed detailed NMR analyses on two such oligosaccharides, a tetrasaccharide (Mikhailov *et al.*, 1996) and a hexasaccharide (Mikhailov *et al.*, 1997). One can estimate the overall conformation of the oligosaccharides using the Iterative Relaxation Matrix Approach (IRMA; Boelens *et al.*, 1988.) to interpret NOE data, followed by refinement using molecular mechanics. This method will, by its very nature, find one single conformation which best fits all the data; subsequent refinement of structures with solvent simulation gives some indication of the extent of internal mobility of the molecule. The glycosidic linkages have similar conformations to their equivalents in the polysaccharide.

An oligosaccharide of particular relevance to the therapeutic importance of heparin is the pentasaccharide at the heart of the naturally-occurring sequence with high affinity for antithrombin (Figure 4c). Ragazzi *et al.* (1987) have performed a molecular mechanics and proton NMR study of a corresponding synthetic pentasaccharide (Figure 4d) which identified several conformations with favorable energy. A dynamics study based on NMR relaxation measurements (Hricovini and Torri, 1995) was consistent with anisotropic reorientation of the molecule and rapid internal motions.

Flexibility of heparin—summary

So far heparin has been presented as displaying both unusual mobility (in the iduronate ring) and unusual rigidity (in the glycosidic conformations and hence the overall molecular shape). Is heparin more or less flexible than other polysaccharides? Perhaps the answer is "differently flexible." Heparin and its derivatives appear to reorient as symmetric tops in solution, implying a rod-like shape. The glycosidic linkages in heparin appear relatively stiff, but the iduronate pyranose rings can adopt at least two conformations. Figure 3 shows how this ring form can change with only a modest effect on the geometry of linkages to the two neighboring residues. Flexibility of the iduronate pyranose ring need not alter the shape of the heparin polysaccharide chain. Thus far, the evidence gathered regarding this conformational change indicates that it is not rapid compared with overall molecular reorientation.

Heparan sulfate

Heparin is easy to obtain, easy to work with, and binds strongly to all or most of the proteins whose physiological ligand is cell-surface heparan sulfate (HS). HS has exactly the same component disaccharides as heparin but in different, and very much more variable, proportions (Figure 4a,b). The unsulfated GlcA-GlcNAc sequence is the most common, with shorter IdoA-containing, sulfated S-regions (Lyon and Gallagher, 1998) of two to nine disaccharides separated on average by sixteen to eighteen mixed or N-acetylated disaccharides. Clearly, the complex sequence patterns of HS do not arise at random (Lindahl *et al.*, 1998). A substantial proportion of the heparan sulfate chain consists of alternating GlcA-GlcNAc, with no sulfate substitution. Given that this sequence has not yet been found to directly influence protein binding, it may function as a spacer between the S-regions.

The most convenient model compound for unsulfated heparan is the capsular polysaccharide of *E.coli* K5. Hricovini *et al.* (1997) have collected carbon relaxation times at several fields for a low molecular weight sample of this polysaccharide and find that the data compare neither with a rigid isotropic motional model, nor with an isotropic model with rapid internal motion. Consideration of the molecule as a symmetric top, with additional rapid internal motions, improves the fit of predicted data to the experimental. Thus far there have been no reported studies of the glycosidic linkage geometries and overall conformation of this sequence.

One can consider the disaccharides maltose and cellobiose as models for the K5/heparan GlcNAc-GlcA and GlcA-GlcNAc linkages respectively. Researchers have identified more than one low-energy linkage conformation for both of these linkage types (Stevens and Sathyanarayama, 1989; Dowd *et al.*, 1992a,b). This would allow the S-regions of heparan sulfate to explore a greater variety of orientations with respect to the attached proteoglycan core than a rigid chain, and would allow two or more S-regions in a single HS chain more freedom to interact with different proteins. The interaction between heparan sulfate and the multimeric form of platelet factor 4 (PF4) is interesting in this regard. Stringer and Gallagher (1997) have described a heparan sulfate fraction with high affinity for PF4, in which two S-regions are separated by a long unsulfated stretch. The length of this stretch of polysaccharide chain is sufficient to present S-regions to binding sites on opposite sides of the PF4 tetramer.

Conformations of heparin oligosaccharides bound to proteins

A large number of heparin-binding proteins has already been identified (Conrad, 1998) and the number continues to increase. Unfortunately, x-ray crystallographic studies exist for only a few heparin-protein complexes: heparin or heparin oligomers complexed with basic fibroblast growth factor (b-fgf; PDB codes 1BFB and 1BFC; Faham *et al.*, 1996), with acidic fibroblast growth factor (a-fgf; 1AXM and 2AXM; DiGabriele *et al.*, 1998), and with foot and mouth disease virus (1QQP; Fry *et al.*, 1999). An additional study features a synthetic heparin-like pentasaccharide (Figure 4e) complexed with both the active and latent members of an antithrombin dimer (1AZX; Jin *et al.*, 1997).

The heparin oligosaccharides bound to growth factors are all derived from multiples of the main trisulfated disaccharide repeat unit (Figure 4a). Faham *et al.* (1996) studied both a tetrasaccharide and hexasaccharide complexed with basic fibroblast growth factor. The conformation of the two iduronate rings in the hexasaccharide complex (1BFC; Faham *et al.*, 1996) is interesting; one adopts the $^{1}C_{4}$ chair, and the other the $^{2}S_{0}$ skew boat (see Figure 3). Lam *et al.* (1998) have used this hexasaccharide/protein complex in a molecular modeling exercise to predict the structure of the multicomponent complex between b-fgf, heparin, and the high-affinity growth factor receptor.

In order to prepare the a-fgf/heparin complex, (1AXM, 2AXM) this study employs a decasaccharide (of which only 5 or 6 monosaccharide units are well-ordered in the crystal structure) sandwiched between two protein molecules. This 2:1 complex illustrates very well the double-sided nature of the heparin molecule, capable of almost identical interactions with two copies of a protein facing each other on either side of the heparin chain.

Fry *et al.* (1999) have determined the crystal structure of foot and mouth virus complexed with polydisperse heparin, as the large dimensions of the crystal can accommodate longer heparin chains than the small fibroblast growth factor proteins. Only five monosaccharide units give sufficiently well-defined electron density to yield coordinates in the PDB file (1QQP), with the outer two residues less well defined than the central three. Electron density for the central iduronate residue fits best to a mixture of $^{1}C_{4}$ and $^{2}S_{0}$ forms. One of the outer iduronates is in the $^{1}C_{4}$ chair, while the other appears to adopt a $^{2,5}B$ conformation (Figure 2). This is the first time experimental evidence for a boat form of iduronate has been reported.

The interaction between heparin and antithrombin differs from all other heparin-protein interactions described thus far. Interestingly, heparin, synthesized in mast cells and sequestered in their granules (Humphries *et al.*, 1999; Forsberg *et al.*, 1999) contains a specific and unusual monosaccharide sequence with a high affinity for the plasma serine protease inhibitor antithrombin. The details of this sequence were first elucidated by Rosenberg and Lam (1979) and by Lindahl *et al.* (1980). Heparin containing this sequence binds to antithrombin and causes a conformational change making it a much more efficient inhibitor of its target serine proteases. Choay *et al.* (1983) have confirmed the structure of this sequence (Figure 4c) by synthesis of its central pentasaccharide (Figure 4d), thus enabling studies of its conformation and dynamics in solution as described above (Ragazzi *et al.*, 1987; Hricovini and Torri, 1995). Other studies investigate antithrombin-tetrasaccharide complexes in the solution state (Figure 4f) (Hricovini *et al.*, 1999) and antithrombin-pentasaccharide complexes in the solid state (Figure 4e) (Jin *et al.*, 1997).

One can compare this crystal structure of an antithrombin/pentasaccharide complex (Jin *et al.*, 1997) with an earlier molecular model prepared by homology modeling and docking calculations informed by biochemical data (Grootenhuis and van Boeckel, 1991). The solid state study (Jin *et al.*, 1997) shows the pentasaccharide occupying the expected binding site, near the predicted orientation, but somewhat displaced; the heparin binding site of antithrombin can accommodate longer oligosaccharide sequences such as a recently studied heptasaccharide (Figure 4g) (Belzar *et al.*, 2000). The bound pentasaccharide has a conformation roughly similar to one of the conformations (designated "S1112") predicted for the pentasaccharide in Figure 4d (Ragazzi *et al.*, 1987); the iduronate residue adopts a conformation between the $^{2}S_{0}$ skew-boat and $^{2,5}B$ forms.

A substantial and complex NMR study of a tetrasaccharide (the methyl glycoside of the sequence AGA*I; Figure 4f) in solution and in the presence of antithrombin (Hricovini *et al.*, 1999) provides a direct comparison of free and bound oligosaccharide. This study describes a distinct change in conformation at the AG glycosidic linkage on binding, and a stabilization of the $^{1}C_{4}$ chair of the iduronate residue. Neither of these conformational features is seen in the pentasaccharide/antithrombin x-ray structure described above; however, the substantial differences in oligosaccharide structure may result in different binding modes within the long heparin binding site of antithrombin.

Figure 6 shows plots of the glycosidic dihedral angles of heparin oligosaccharides bound to fibroblast growth factors and to foot and mouth virus, together with values from NMR studies of heparin and of a heparin oligosaccharide. The similar glycosidic bond geometries of all these structures corroborates the idea that heparin has a well-defined conformation both in solution and in the solid state. The presence of skew-boat (1BFC), boat (1QQP), and intermediate (1AZX) ring forms of iduronate in crystals indicates the accessibility of these forms and lends weight to the idea that such conformations may exist in solution.

In principle, one can predict the location of heparin-binding sites on proteins using the geometry of heparin as a guide. Cardin and Weintraub (1989) first defined heparin-binding motifs in protein primary sequences such as XBBBXXBX and XBBXBX (where B is a basic residue and X a hydropathic residue). These motifs, in the context of their secondary structure, are capable of presenting clusters of basic residues towards the heparin molecule. Combination of this sequence-based approach (reviewed recently by Hileman *et al.*, 1998) with extra geometrical information allows identification of discontinuous heparin-binding sites. The distance between sulfate clusters along one side of the heparin, about 17Å, approximately matches the periodicity of a right-handed α-helix, consistent with the ability of heparin to induce α-helix in polylysine (Mulloy *et al.*, 1996). It also approximates the 20 Å dimension identified as typical of heparin binding sites in proteins (Margalit *et al.*, 1993). Any protein with a patch of basic residues on its surface will interact with the highly acidic heparin; identification of two patches of basic residues with a spacing of about 17Å between them would serve as a first step towards a structurally specific binding site. Najjam *et al.* (1998) have used this simple, manual technique to define a proposed site on interleukin-2. A more systematic procedure employs a computational docking technique. Bitomsky and Wade (1999) report on the use of several different software options for this approach, and we have found in our own work that heparin pentasaccharide probes based on the NMR structure can predict the position of binding sites with remarkable accuracy (Figure 7).

Heparin binds tightly to some proteins, such as the fibroblast growth factors, increasing affinity for the receptor, and forming part of the receptor complex on the cell surface; the interaction is only partly coulombic and incorporates nonionic

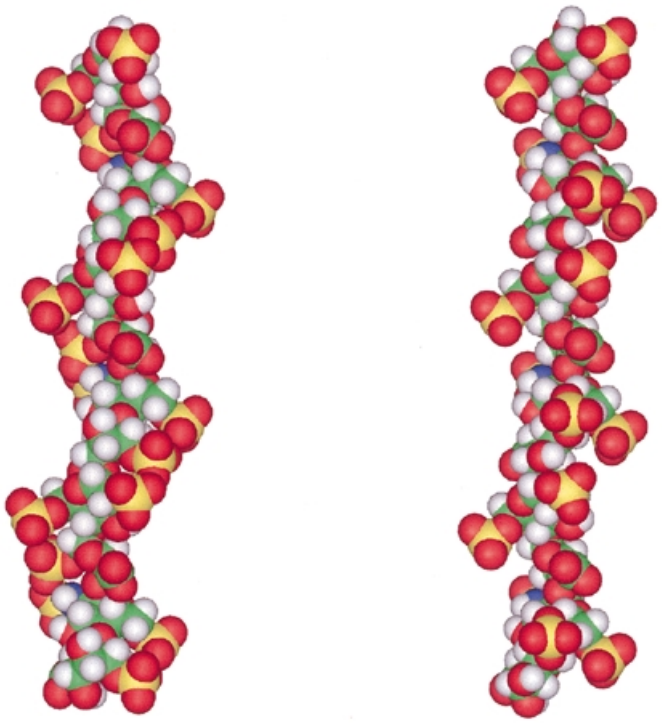

Fig. 5. A solution structure of heparin determined by NMR (Mulloy *et al.*, 1993). The iduronate is displayed as (**a**) $^{1}C_{4}$ chair and (**b**) $^{2}S_{0}$ skew-boat, to display the conformational consequences of the interconversion; there is no suggestion that all the iduronates in a single molecule change form in a concerted fashion.

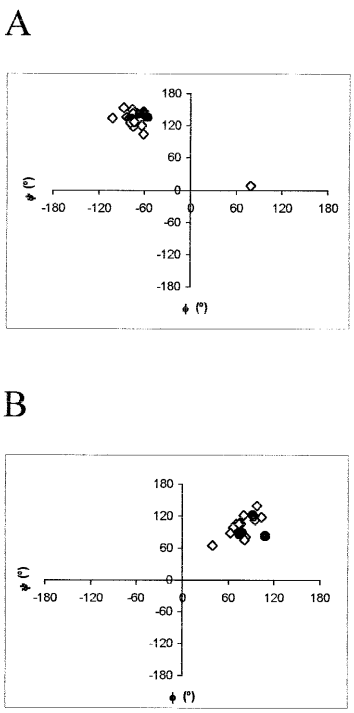

Fig. 6. Plots of the glycosidic dihedral angles for A) α-L-IdoA2(OSO_3^-)-(1→4)-α-D-GlcNSO_3^-,6(OSO_3^-) and B) α-D-GlcNSO_3^-,6(OSO_3^-)-(1→4)- α-L-IdoA2(OSO_3^-) in complexed crystal structures 1AXM, 2AXM, 1BFB, 1BFC, and 1QQP (lozenge) and solution NMR structures 1HPN and according to (Mikhailov *et al.*, 1996, 1997) (solid circle). The atoms defining ϕ are O5′-C1′-O4-C4 and ψ are C1′-O4-C4-C3. There is a considerable degree of agreement between almost all published structures.

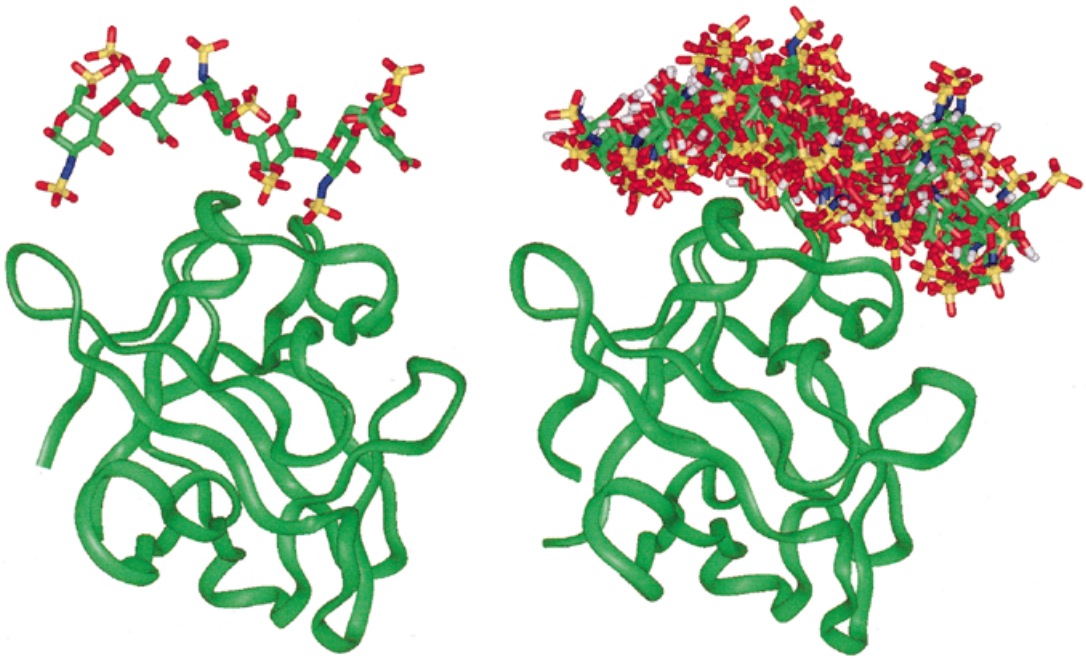

Fig. 7. The x-ray structure of the complex of basic fgf with a heparin hexasaccharide (pdb code 1BFC) is shown on the left. The right-hand side of the figure shows a structure for a non-complexed form of basic fgf (pdb code 2FGF) and the best twenty predicted binding sites for a set of heparin pentasaccharide probe molecules. The docking predictions were performed with Autodock version 2.4 (Oxford Molecular Inc). The heparin probe molecules used have conformations derived from the reported NMR structure (pdb code 1HPN). Separate docking calculations were performed using probe molecules in which the iduronate residues adopt the $^{1}C_{4}$ and $^{2}S_{0}$ ring forms. The 20 complexes shown are those with the top ten scores for each form of probe molecule.

interactions (Thompson *et al.*, 1994; Faham *et al.*, 1996). Other heparin–protein interactions are more heavily electrostatic in nature, and of more moderate affinity. Lander (1998) argues that heparin and heparan sulfate may be capable of acting as "catalysts of molecular interaction," affecting the kinetics of interaction without altering thermodynamics. The prime example of this role is that of heparin and antithrombin. Heparin accelerates binding between antithrombin and its serine protease targets, and once the protein–protein complex is formed it is released intact. There may well be many more such instances. Heparin and the protein-binding regions of heparan sulfate display a defined overall shape in which variations of sulfate substitution and iduronate flexibility are capable of providing a range of finely tuned affinities for different proteins in different circumstances. GAGs such as heparin and heparan sulfate could therefore play a part in complex control mechanisms particularly suited to processes very far from equilibrium, such as growth and differentiation.

Summary and conclusions

Heparin structures have now been reported in the solution and solid states as well as in complexes with a number of proteins. Analysis of these data indicates that the conformation of heparin is well-defined with similar glycosidic torsional angles found in almost all cases. Within this overall conformation, the pyranose rings of iduronate residues have significant flexibility. In solution they exist in a dynamic equilibrium, and when complexed with proteins can adopt several different forms. Studies of solution structure for heparin and its derivatives must take account of internal motion, and allow for averaging over several conformational states of NMR measurements such as NOEs. The relative timescales of internal and overall molecular motions must also be borne in mind. Variations in sulfate substitution affect the conformational equilibrium of the iduronate ring more than the overall shape of the heparin molecule.

There is, so far, less information available for the glucuronate-containing regions of heparan sulfate and heparin; glucuronate residues lack the flexibility of iduronate.

Molecular modeling exercises for heparin and heparan/protein complexes require care in the choice of strategy and parametrization of any force-field used. However, the well-defined shape of heparin molecules increases the value of predictive molecular modeling exercises.

Abbreviations

GAG, glycosaminoglycan; NOE, Nuclear Overhauser effect; a-fgf, acidic fibroblast growth factor FGF-I; b-fgf, basic fibroblast growth factor FGF-II

References

Asensio,J.L., Martin-Pastor,M. and Jimenez-Barbero,J. (1995) The use of CVFF and CFF91 force-fields in conformational analysis of carbohydrate molecules. Comparison with AMBER molecular mechanics and dynamics calculations for methyl α-lactoside. *Int. J.Biol. Macromol.*, **17**, 137–148.

Atkins,E.D. and Nieduszynski,I.A. (1975) Crystalline structure of heparin. *Adv. Exp. Med. Biol.*, **52**, 19–37.

Belzar,K.J., Dafforn,T.R., Petitou,M., Carrell,R.W. and Huntington,J.A. (2000) The effect of a reducing-end extension on pentasaccharide binding by antithrombin. *J. Biol. Chem.*, **275**, 8733–8741.

Bitomsky,W. and Wade,R. (1999) Docking of glycosaminoglycans to heparin-binding proteins: validation for aFGF, bFGF and antithrombin and application to IL-8. *J. Am. Chem. Soc.*, **121**, 3004–3013.

Boelens,R., Koning,T.M.G. and Kaptein, R (1988) Determination of biomolecular structures from proton-proton NOEs using a relaxation matrix approach. *J. Mol. Struct.*, **173**, 299–311.

Brunger,A.T. and Nilges,M. (1990) Computational challenges for macromolecular structure determination by x-ray crystallography and solution NMR-spectroscopy. *J. Mol. Biol.*, **214**, 223–35

Cardin,A.D. and Weintraub,H.J. (1989) Molecular modeling of protein-glycosaminoglycan interactions. *Arteriosclerosis*, **9**, 21–32.

Catoire,L., Braccini,I., Bouchemal-Chibani,N., Jullien,L., Herve du Penhoat,C. and Perez,S. (1997) NMR analysis of carbohydrates with model-free spectral densities: the dispersion range revisited. *Glycoconj J.*, **14**, 935–943.

Choay,J., Lormeau,J.C., Petitou,M., Sinay,P. and Fareed,J. (1981) Structural studies on a biologically active hexasaccharide obtained from heparin. *Ann. N.Y. Acad. Sci.*, **370**, 644–649.

Choay,J., Petitou,M., Lormeau,J.C., Sinay,P., Casu,B. and Gatti,G. (1983) Structure-activity relationship in heparin: a synthetic pentasaccharide with high affinity for antithrombin III and eliciting high anti-factor Xa activity. *Biochem. Biophys. Res. Commun.*, **116**, 492–499.

Conrad,H.E. (1998) *Heparin-Binding Proteins*. Academic Press, San Diego.

Cremer,D. and Pople,J.A. (1975) A general definition of ring puckering coordinates. *J. Am. Chem. Soc.*, **97**, 1354–1358.

Cumming,D.A. and Carver,J.P. (1987) Virtual and solution conformations of oligosaccharides. *Biochemistry*, **26**, 6664–76.

DiGabriele,A.D., Lax,I., Chen,D.I., Svahn,C.M., Jaye,M., Schlessinger,J. and Hendrickson,W.A. (1998) Structure of a heparin-linked biologically active dimer of fibroblast growth factor. *Nature*, **393**, 812–817.

Dowd,M.K., French,A.D. and Reilly,P.J. (1992a) Conformational analysis of the anomeric forms of sophorose, laminarabiose and cellobiose using MM3. *Carbohydr. Res.*, **233**, 15–34.

Dowd,M.K., Zeng,J., French,A.D. and Reilly,P.J. (1992b) Conformational analysis of the anomeric forms of kojibiose, nigerose and maltose using MM3. *Carbohydr. Res.*, **230**, 223–244.

Ernst,S., Venkataraman,G., Sasisekharan,V., Langer,R., Cooney,C.L. and Sasisekharan,R. (1998) Pyranose ring flexibility. Mapping of physical data for iduronate in continuous conformational space. *J. Am. Chem. Soc.*, **120**, 2099–2107.

Faham,S., Hileman,R.E., Fromm,J.R., Linhardt,R.J. and Rees,D.C. (1996) Heparin structure and interactions with basic fibroblast growth factor. *Science*, **271**, 1116–1120.

Ferro,D.R., Provasoli,A., Ragazzi,M., Casu,B., Torri,G., Bossennec,V., Perly,B., Sinay,P., Petitou,M. and Choay,J. (1990) Conformer populations of L-iduronic acid residues in glycosaminoglycan sequences. *Carbohydr. Res.*, **195**, 157–167.

Ferro,D.R., Pumilia,A., Cassarini,A. and Ragazzi,M. (1995a) Treatment of ionic species in force field calculations: sulfate and carboxylate groups in carbohydrates. *J. Comp. Chem.*, **17**, 131–135.

Ferro,D.R., Gajdos,J., Ragazzi,M., Ungarelli,F. and Piani,S. (1995b) Conformational analysis of heparin epoxide: molecular mechanics computations. *Carbohydr. Res.*, **277**, 25–28.

Ferro,D.R., Pumilia,A. and Ragazzi,M. (1997) An improved force field for conformational analysis of sulfated polysaccharides. *J. Comp. Chem.*, **18**, 351–367.

Forsberg,E., Pejler,G., Ringvall,M., Lunderius,C., Tomasini-Johansson,B., Kusche-Gullberg,M., Eriksson,I., Ledin,J., Hellman,L. and Kjellen,L. (1999) Abnormal mast cells in mice deficient in a heparin-synthesizing enzyme. *Nature*, **400**, 773–776.

Forster,M.J. and Mulloy,B. (1993) Molecular dynamics study of iduronate ring conformation. *Biopolymers*, **33**, 575–588.

Forster,M.J. and Mulloy,B. (1994) Rationalizing nuclear Overhauser effect data for compounds adopting mutiple-solution conformations. *J. Comp. Chem.*, **15**, 155–161.

Forster,M., Jones,C. and Mulloy,B. (1989) NOEMOL: integrated molecular graphics and the simulation of Nuclear Overhauser effects in NMR spectroscopy. *J. Mol. Graph.*, **7**, 196–201.

Fry,E.E., Lea,S.M., Jackson,T., Newman,J.W., Ellard,F.M., Blakemore,W.E., Abu-Ghazaleh,R., Samuel,A., King,A.M. and Stuart,D.I. (1999) The structure and function of a foot-and-mouth disease virus-oligosaccharide receptor complex. *EMBO J.*, **18**, 543–554.

Gatti,G., Casu,B., Hamer,G.K. and Perlin,A.S. (1979) Studies on the conformation of heparin by 1H and 13C NMR spectroscopy. *Macromolecules*, **12**, 1001–1007.

Grootenhuis,P.D.J. and van Boeckel,C.A. (1991) Constructing a molecular model of the interaction between antithrombin III and a potent heparin analogue. *J. Am. Chem. Soc.*, **113**, 2743–2747.

Hadjuk,P.J., Horita,D.A. and Lerner,L.E. (1993) Picosecond dynamics of simple monosaccharides as probed by NMR and molecular dynamics simulations. *J. Am. Chem. Soc.*, **115**, 9196–9201.

Hagner-McWhirter,A., Lindahl,U. and Li,J. (2000) Biosynthesis of heparin/heparan sulphate: mechanism of epimerization of glucuronyl C-5. *Biochem J.*, **347**, 69–75.

Harris,R.K. (1986) *Nuclear Magnetic Resonance Spectroscopy: A Physicochemical View*. Addison-Wesley, Reading, MA.

Hileman,R.E., Fromm,J.R., Weiler,J.M. and Linhardt,R.J. (1998) Glycosaminoglycan-protein interactions: definition of consensus sites in glycosaminoglycan binding regions. *Bioessays*, **20**, 156–167.

Horita,D.A., Hajduk,P.J. and Lerner,L.E. (1997) Solution dynamics of the 1,2,3,4,6-penta-O-acetyl-alpha-D-idopyranose ring. *Glycoconj. J*, **14**, 691–696.

Hricovini,M., Guerrini,M., Torri,G. and Casu,B. (1997) Motional properties of *E. coli* polysaccharide K5 in aqueous solution analyzed by NMR relaxation measurements. *Carbohydr. Res.*, **300**, 69–76.

Hricovini,M. and Torri,G. (1995) Dynamics in aqueous solutions of the pentasaccharide corresponding to the binding site of heparin for antithrombin III studied by NMR relaxation measurements. *Carbohydr. Res.*, **268**, 159–175.

Hricovini,M., Guerrini,M., Torri,G., Piani,S. and Ungarelli,F. (1995) Conformational analysis of heparin epoxide in aqueous solution. An NMR relaxation study. *Carbohydr. Res.*, **277**, 11–23.

Hricovini,M., Guerrini,M. and Bisio,A. (1999) Structure of heparin-derived tetrasaccharide complexed to the plasma protein antithrombin derived from NOEs, J-couplings and chemical shifts. *Eur. J. Biochem.*, **261**, 789–801.

Huckerby,T.N. and Nieduszynski,I.A. (1982) Investigation of ^{13}C relaxation and nuclear overhauser enhancement parameters for heparinoid systems: comparison with data for dextrans. *Int. J. Biol. Macromol.*, **4**, 269–274.

Huige,C.J. and Altona,C. (1995) Force field parameters for sulfates and sulfamates based on *ab initio* calculations: extensions of AMBER and CHARMm fields. *J. Comp. Chem.*, **16**, 56–79.

Humphries,D.E., Wong,G.W., Friend,D.S., Gurish,M.F., Qiu,W.T., Huang,C., Sharpe,A.H. and Stevens,R.L. (1999) Heparin is essential for the storage of specific granule proteases in mast cells. *Nature*, **400**, 769–772.

Jeffrey,G.A. and Yates,J.H. (1979) Stereographic representation of the Cremer-Pople ring-puckering parameters for pyranoid rings. *Carbohydr. Res.*, **74**, 319–322.

Jin,L., Abrahams,J.P., Skinner,R., Petitou,M., Pike,R.N. and Carrell,R.W. (1997) The anticoagulant activation of antithrombin by heparin. *Proc. Natl. Acad. Sci. USA*, **94**, 14683–14688.

Lam,K., Rao,V.S. and Qasba,P.K. (1998) Molecular modeling studies on binding of bFGF to heparin and its receptor FGFR1. *J. Biomol. Struct. Dyn.*, **15**, 1009–1027.

Lander,A. (1998) Proteoglycans: master regulators of molecular encounter? *Matrix Biol.*, **17**, 465–472.

Lindahl,U., Backstrom,G., Thunberg,L. and Leder,I.G. (1980) Evidence for a 3-O-sulfated D-glucosamine residue in the antithrombin-binding sequence of heparin *Proc. Natl Acad. Sci. USA*, **77**, 6551–6555.

Lindahl,U., Kusche-Gullberg,M. and Kjellen,L. (1998) Regulated diversity of heparan sulfate. *J. Biol. Chem.*, **273**, 24979–24982.

Lipari,G. and Szabo,A. (1982a) Model-free approach to the interpretation of nuclear magnetic resonance relaxation in macromolecules. 1. Theory and range of validity. *J. Am. Chem. Soc.*, **104**, 4546–4559.

Lipari,G. and Szabo,A. (1982b) Model-free approach to the interpretation of nuclear magnetic resonance relaxation in macromolecules. 2. Analysis of experimental results. *J. Am. Chem. Soc.*, **104**, 4559–4570.

Lyon,M. and Gallagher,J.T. (1998) Bio-specific sequences and domains in heparan sulphate and the regulation of cell growth and adhesion [see comments]. *Matrix Biol.*, **17**, 485–493.

Margalit,H., Fischer,N. and Ben-Sasson,S.A. (1993) Comparative analysis of structurally defined heparin binding sequences reveals a distinct spatial distribution of basic residues. *J. Biol. Chem.*, **268**, 19228–19231.

McCammon,J.A. and Harvey,S.C. (1987) *Dynamics of Proteins and Nucleic Acids*. Cambridge University Press, Cambridge.

Mikhailov,D., Mayo,K.H., Vlahov,I.R., Toida,T., Pervin,A. and Linhardt,R.J. (1996) NMR solution conformation of heparin-derived tetrasaccharide. *Biochem. J.*, **318**, 93–102.

Mikhailov,D., Linhardt,R.J. and Mayo,K.H. (1997) NMR solution conformation of heparin-derived hexasaccharide. *Biochem. J.*, **328**, 51–61.

Mulloy,B., Crane,D.T., Drake,A.F. and Davies,D.B. (1996) The interaction between heparin and polylysine: a circular dichroism and molecular modeling study. *Braz. J. Med. Biol. Res.*, **29**, 721–729.

Mulloy,B., Forster,M.J., Jones,C. and Davies,D.B. (1993) N.m.r. and molecular-modeling studies of the solution conformation of heparin. *Biochem. J.*, **293**, 849–858.

Mulloy,B., Forster,M.J., Jones,C., Drake,A.F., Johnson,E.A. and Davies,D.B. (1994) The effect of variation of substitution on the solution conformation of heparin: a spectroscopic and molecular modeling study. *Carbohydr. Res.*, **255**, 1–26.

Najjam,S., Mulloy,B., Theze,J., Gordon,M., Gibbs,R. and Rider,C.C. (1998) Further characterization of the binding of human recombinant interleukin 2 to heparin and identification of putative binding sites. *Glycobiology*, **8**, 509–516.

Perez,S., Imberty,A.,. Engelsen,S.B., Gruza,J., Mazeau,K., Jimenez-Barbero,J., Poveda,A., Espinosa,J., van Eyck,B.P., Johnson,G. and others. (1998) A comparison and chemometric analysis of several molecular mechanics force fields and parameter sets applied to carbohydrates. *Carbohydr. Res.*, **314**, 141–155.

Ragazzi,M., Ferro,D.R., Perly,B., Torri,G., Casu,B., Sinay,P., Petitou,M. and Choay,J. (1987) Conformation of the pentasaccharide corresponding to the binding site of heparin to antithrombin-III. *Carbohydr. Res.*, **165**, c1-c5

Rao,V.S.R., Qasba,P.K., Balaji,P.V. and Chandrasekaran,R. (1998) *Conformation of Carbohydrates*, Harwood Academic, Amsterdam.

Rosenberg,R.D. and Lam,L. (1979) Correlation between structure and function of heparin. *Proc. Natl. Acad. Sci. USA*, **76**, 1218–1222.

Rutherford,T.J., Partridge,J., Weller,C.T. and Homans,S.W. (1993) Characterization of the extent of internal motions in oligosaccharides. *Biochemistry*, **32**, 12715–12724.

Sanderson,P.N., Huckerby,T.N. and Nieduszynski,I.A. (1987) Conformational equilibria of α-L-iduronate residues in disaccharides derived from heparin. *Biochem. J.*, **243**, 175–181.

Snyder,J.R. and Serianni,A.S. (1986) D-Idose: a one- and two-dimensional NMR investigation of solution composition and conformation. *J. Org. Chem.*, **51**, 2694–2702.

Stevens,E.S. and Sathyanarayama B.K. (1989) Potential energy surfaces of cellobiose and maltose in aqueous solution: a new treatment of disaccharide optical rotation. *J. Am. Chem. Soc.*, **111**, 4149–4154.

Stringer,S.E. and Gallagher,J.T. (1997) Specific binding of the chemokine platelet factor 4 to heparan sulfate. *J. Biol. Chem.*, **272**, 20508–20514.

Thompson,L.D., Pantoliano,M.W. and Springer,B.A. (1984) Energetic characterization of the basic fibroblast growth factor-heparin interaction: identification of the heparin binding domain. *Biochemistry*, **33**, 3831–3840.

van Boeckel,C.A., van Aelst,S.F., Wagenaars,G.N., Mellema,J.-R., Paulsen,H., Peters,T., Pollex,A. and Sinnwell,V. (1987) Conformational analysis of synthetic heparin-like oligosaccharides containing α-L-idopyranosyluronic acid. *Recl. Trav. Pays-Bas*, **106**, 19–29.

Wagner,G., Braun,W., Havel,T.F., Schaumann,T., Go,N. and Wuthrich,K. (1993) Protein structures in solution by nuclear magnetic resonance and distance geometry. The polypeptide fold of the basic pancreatic trypsin inhibitor determined using two different algorithms, DISGEO and DISMAN. *Q. Rev. Biophys.* **26**, 49–125.

Wuthrich,K. (1986) *NMR of Proteins and Nucleic Acids*, Wiley, New York,

Xu,Q., Mohan,S. and Bush,C.A. (1996) A flexible model for the cell wall polysaccharide of Streptococcus mitis J22 determined by three-dimensional ^{13}C edited nuclear overhauser effect spectroscopy and ^{13}C-^{1}H long-range coupling constants combined with molecular modeling. *Biopolymers*, **38**, 339–353.